Paper IV
Gene expression profiles of human bone marrow stromal cells co-cultured with endothelial cells. (*Manuscript*)

IV

Gene expression profiles of human bone marrow stromal cells co-cultured with endothelial cells

Ying Xue [1], Anne Isine Bolstad [2], Sølve Hellem [3], Kristina Arvidson [1], Kamal Mustafa [1]

Authors' affiliations:

[1]Department of Clinical Dentistry-Center for Clinical Dental Research, University of Bergen, Norway

[2]Department of Clinical Dentistry - Periodontology, University of Bergen, Bergen, Norway

[3]Department of Clinical Dentistry - Oral and Maxillofacial Surgery, University of Bergen, Bergen, Norway

Abstract:

There is an intricate relationship between angiogenesis and osteogenesis *in vivo* and failure to simulate this relationship in bone tissue engineering constructs, by ensuring a functional vascular network, is a major obstacle to successful bone formation. Although communication between bone marrow stromal cells (MSC) and endothelial cells (EC) is recognized as one of the most important cellular interactions in bone formation, the underlying mechanisms are not well understood. The aim of this study was to analyze patterns of global gene expression associated with so-called cross-talk between MSC and EC, using HumanWG-6 v3.0 expression BeadChips with a one-channel Illumina platform system. Each array represents more than 48,000 probes derived from human genes. A global map of gene expression was generated, representing interactions between MSC and EC following co-culture for 5 and 15 days respectively, in a direct-contact model. The map was used to determine relative functional processes and pathways. The results indicated that EC had a significant impact on MSC, particularly the bidirectional gene regulation of angiogenesis and osteogenesis, mainly through cell signalling, cell adhesion and the cellular matrix. Cell-matrix interactions and TGF-beta signal pathways might play crucial roles in endothelial cell-induced gene regulation of MSC. More detailed study of the microarray data is warranted to explore further possible cellular and molecular interactions of importance in bone tissue engineering.

Introduction

The limitations associated with treatment of bone defects by autografts and allografts have led to intensified efforts to develop alternative approaches, based on the principles of bone tissue engineering [1]. It is crucial that on implantation, the engineered has a fully functional vascular network: this remains a major obstacle to clinical application [2].

It is well known that limited ingrowth of blood vessels into the transplanted grafts will gradually occur, due to hypoxia. In order to receive oxygen and nutrients through diffusion, cells must be located within 100-200 μm of a blood vessel.

Bone is formed by two distinct modes of ossification [3]: intramembranous and endochondral. In intramembranous bone formation there is an invasion of capillaries for the transport of mesenchymal stem cells, which can differentiate directly into osteoblasts and in turn secret bone matrix. In endochondral ossification, MSC first differentiate into chondroblasts to form a framework of cartilage, and then induce the invasion of blood vessels, bringing a number of specialized cells to replace the cartilage with bone and bone marrow. Another important role of vascularization in bone formation is the production of growth factors which control the recruitment, proliferation, differentiation, function, and/or survival of bone cells. Therefore, angiogenesis not only precedes osteogenesis but is also essential for its occurrence.

Because of the intricate association between angiogenesis and osteogenesis *in vivo*, communication between bone marrow stromal cells (MSC) and endothelial cells (EC) represents one of the most important cellular interactions for bone formation [2]. Previous studies have shown that co-culture with endothelial cells enhances cellular proliferation of MSCs and induces osteogenic differentiation, such as up-regulation of alkaline phosphatase (ALP) expression [4, 5]. It has been reported that EC co-cultured with osteoblasts (OB) are able to establish microcapillary-like structures in a 3D scaffold. Both MSC and the endothelial

network express connexion 43 (Cx43), a specific gap junction protein. These two cell types can therefore communicate via a gap junctional channel comprising Cx43 [4].

In support of these *in vitro* communication studies, *in vivo* studies have also shown beneficial effects of using co-cultures of EC and OB in tissue-engineering constructs. For example, in a rat model, a construct comprising endothelial progenitor cells and bone marrow-derived osteoblasts, co-cultured on PCL scaffolding, was implanted into calvarial defects: the results revealed not only improved osteogenesis but also enhanced vascularization [6]. Co- cultured OB and EC within RGD-grafted alginate microspheres in a long bone defect of mice showed significantly enhanced mineralization of the microspheres [2]. In vivo, bone regeneration was enhanced by a construct of the polymer scaffold loaded with co-cultured cells [7].

The above studies show that EC can influence not only osteogenic differentiation *in vitro,* but also osteogenesis *in vivo*. As so-called cross-talk between MSC and EC was identified as one of the most important cellular interactions coordinating the bone regeneration process, new and multidisciplinary approaches are needed for more detailed investigation of these cellular interactions.

Microarray-based global gene expression profiling constitutes a valuable research tool for ascertaining the varying patterns of gene expression in relation to co-cultured MSC and EC.

In this context, the aim of the present study was to analyse patterns of global gene expression associated with cross-talk between human MSC and EC. The HumanWG-6 v3.0 expression BeadChips system was used, with the Illumina one-channel platform system. Each array represents >48,000 probes, derived from human genes in the NCBI RefSeq and UniGene databases and provides genome-wide transcriptional coverage of well-characterized genes, gene candidates, and splice variants.

Materials and Methods

Experimental Design

In order to carry out a systematic assessment of the impact of co-culture on MSC, the experiments used MSC from six different individuals: the cells were treated with mixed EC at a ratio of 5:1 and the same donor. Monocultured MSC served as controls. Two time points, 5 and 15 days, were chosen for the experiments. The material at each time point comprised six samples in the co-culture group (T) and six in the control group (C), giving 24 samples in all. All six cell samples were sourced from different donors (Table 1) and denoted D1-D6. The sample from donor X in the co-culture group was paired with the sample from donor X in the control group.

The microarray platform chosen was Illumina, a one-channel system. The HumanWG-6 v3.0 Expression BeadChips system was used. The 1-channel nature of the platform yields the simple design of 1 sample hybridized to 1 array on a microarray slide. This particular chip has six arrays on each slide.

Cell culture and maintenance

Primary human MSC (StemCell Technologies, Vancouver, BC, Canada) were cultured in MesenCult® complete medium (StemCell Technologies) following the manufacturer's instructions. Cell purity was confirmed by flow cytometry, which showed that > 90% of the cells expressed CD29, CD44, CD105, CD166; < 1% expressed CD14, CD34 and CD45.

Primary human umbilical vein endothelial cells were obtained from Lonza (Clonetics®,Walkersville, MD). In accordance with the manufacturer's instructions, the cells were expanded in EGM Medium (Clonetics® EGM®) containing 500 ml of Endothelial Cell Basal Medium and the following growth supplements: BBE, 2 ml; hEGF, 0.5 ml;

Hydrocortisone, 0.5 ml; FBS, 10 ml; GA-1000, 0.5 ml. For both cell types, passages under 4 were used.

EC and MSC were collected and then mixed in 6-well plates (Nunclon, Roskilde, Denmark) at a ratio of 1:5. The cell density was $2\times10^3/cm^2$ EC and $1\times10^4/cm^2$ MSC in a mixed medium. MSCs were seeded onto 6-well plates as controls. The culture medium was changed after 3 days. Due to the different adherent properties of MSC and EC, EC can be separated by two-step trypsinization. After cultivation for 5 and 15 days, EC in the co-culture group was removed by treatment with 1 ml trypsin/EDTA for 5 min at 37°C. The floating cells were washed away by phosphate buffered saline (PBS). In order to avoid a confounding effect, the control MSC was treated similarly. Finally, the cells were rinsed with 1 ml trypsin for 5 min at 37°C. Following a 5 min centrifuge, MSC were collected from test and control groups. The cell pellets were stored at -80°C until RNA extraction.

Total RNA preparation and quality control

Total RNA was isolated from 5 and 15-day-old cultures, using E.Z.N.A.^{TM} Tissue RNA isolation kit (Omega Bio-Tek, Norcross, GA), according to the manufacturer's protocol. In brief, cells were disrupted by TRK lysis buffer and homogenized. 70% ethanol was then added to the cleared lysate and applied to a HiBind® RNA spin column placed in a 2 ml collection tube. After centrifuging and washing, on-membrane DNase I digestion was performed and RNA was eluted with Nuclease-free water. RNA was quantified using a NanoDrop ND-1000 Spectrophotometer (ThermoScientific NanoDrop Technologies, Wilmington, DE).

RNA integrity is a critical step in obtaining high quality gene expression data. RNA quality was analysed with the Agilent 2100 Bioanalyzer and an electropherogram of each sample was obtained. This bioanalysis yields an RNA Integrity Number (RIN), the value which indicates the quality of the RNA. RIN values range from 1, indicating degraded RNA, to 10 which

indicates perfect RNA. In this study, only samples with a RIN value of at least 7.5 were included in the microarray experiments.

RNA labelling, amplification and microarray hybridisation

250 ng of total RNA from each sample was reversely transcribed, amplified and Biotin-16-UTP–labelled, using the Illumina TotalPrep RNA Amplification Kit (Applied Biosystems/Ambion, USA). The amount and quality of the Biotin-labelled cRNA were controlled by both the NanoDrop spectrophotometer and the Agilent 2100 Bioanalyzer. The Illumina TotalPrep RNA Amplification Kit generates biotinylated, amplified RNA for hybridization with Illumina Sentrix arrays. The procedure consists of reverse transcription with an oligo(dT) primer bearing a T7 promoter using a reverse transcriptase. The reverse transcriptase catalyzes the synthesis of virtually full-length cDNA. The cDNA then undergoes second strand synthesis and clean-up to become a template for *in vitro* transcription with T7 RNA Polymerase. *In vitro* transcription is used to generate hundreds to thousands of biotinylated, antisense RNA copies of each mRNA in a sample.

The biotin-labelled cRNA was hybridized to the HumanWG-6 v3.0 Expression BeadChip which targets >48 000 probes derived from human genes in NCBI RefSeq and UniGene databases. Hybridization was performed according to the Whole-Genome Gene Expression Direct Hybridization Assay Guide from Illumina Inc. 1500 ng cRNA was hybridized at 58˚C for 17 hours. By adding streptavidin-Cy3 after hybridization and washing, the signals can be detected by the Illumina iScan Reader.

Data normalization and quality control

For quality control, the data from the scanning of arrays on the Illumina iScan Reader were evaluated by GenomeStudio and J-Express 2009.

After scanning, the raw data were imported into GenomeStudio and several different quality

control steps were undertaken. Seven different control categories were built into the Whole-Genome Gene Expression Direct Hybridization Assay system. These covered every aspect of an array experiment, from the biological specimen to sample labelling, hybridization, and signal generation. The GenomeStudio application automatically tracks the performance of these controls and generates a report for each array in the matrix. Checking by the full range of technical controls in GenomeStudio confirmed that all the samples were of high quality. The variation between samples was no greater than expected. All samples had a signal-to-noise ratio well above the threshold value of 10. Before being compiled into an expression profile data matrix, all arrays within each experiment were quantile normalized to be comparable.

Microarray Data Analysis

The SampleProbeProfile was loaded into J-Express as two separate experiments: 5- and 15-days.

A box plot is one means of visualizing the distribution of intensities for all arrays. These distributions need to be similar for the different samples to be comparable (Figure 1). Samples which behave differently from the other samples, regardless of biology are denoted outliers and can be detected by clustering and/or projection: these two methods can also be applied to detect batch effects (Figure 2).

To identify differentially expressed genes between two groups, J-express software was used for significance analysis of microarrays (SAM) (Tusher et al) [8]. SAM is a statistical technique for finding significant genes in a set of microarray experiments. Since a donor-paired group was used in this experiment, gene expression measurements were analysed by a paired SAM method. SAM computes a statistic di for each gene i, measuring the strength of the relationship between gene expression and treatment. Repeated permutations of the data were used to determine whether expression of any genes was significantly related to the co-

culture treatment. In the current study, changes in gene-expression profile were identified at an estimated false discovery rate (FDR) of less than 1%. Genes with a fold change of greater than 2 were selected. Differentially expressed genes were mapped to a gene ontology (GO) directed acyclic graph in J-express 2009 and compared with the total number of genes to determine the over-representation of GO terms.

Identification of significantly overrepresented functions

To classify each cluster in more detail by their ontological properties, lists of overrepresented genes from the SAM test were submitted to the Database for Annotation, Visualization and Integrated Discovery (DAVID) [9, 10]. The Gene Functional Classification tool in DAVID builds clusters of genes with significantly similar ontology as tested against the whole list of genes in the Human Genome array. Medium stringency was used to yield a comprehensive set of ontological groups and to group genes with similar functions. Increasing or decreasing stringency resulted in identification of fewer or more groups of genes with similar functions, but did not produce any additional information.

A similar analysis was performed against a reference list of genes through the DAVID bioinformatics database, a classification system (http://www.DAVID.org/) intended to identify overrepresented biological processes and key pathways.

Validation microarray data by RT-PCR

In order to validate the microarray data, quantitative real time PCR was performed on selected up- and down-regulated genes, using TaqMan gene expression assays: Hs00863478_g1 (FLG), Hs00362607_m1 (CD 93), Hs00173787_m1 (CALCRL), Hs00169795_m1 (VWF), Hs01029142_m1 (ALP), Hs00231692_m1 (RunX2), Hs00164099_m1 (Col IA1), and TaqMan Pre-Developed Assay GAPDH (4333764T). cDNA, corresponding to 6 ng of mRNA, was used in each PCR reaction. Mixtures were made up according to the manufacturer's instructions, in 10µl triplicates for each target cDNA.

Amplification was carried out in 96-well thermal cycle plates on a StepOne detection system (Applied Biosystems, USA) according to the manufacturer's recommendations. Gene expression was determined by the comparative Ct method, normalizing expression to the reference gene GADPH. For quantitative RT-PCR, the difference between groups was assessed using ANOVA, with a p-value of less than 0.05 considered to be statistically significant.

Results

Global effects analysis by Hierarchical Clustering and Correspondence Analysis plots

Before differential expression analysis, global visualization of an experiment can be helpful for designing subsequent analysis and for quality control. In all, 48803 genes were identified from the whole data set. In the box plot (Figure 1), un-normalized data show that the distribution varies among the different samples, suggesting that the data should be normalized to make them more comparable. After quantile-normalization, all arrays within each experiment had the same distribution of data, and could now be compared.

The global effects at the two different time points were investigated in two different ways: Hierarchical Clustering (HC) (Figure 2, right) and Correspondence Analysis (CA)-plots (Figure 2, left). In the 5-day experiment, two main clusters were disclosed (Figure 2A). The two clusters correspond to the co-culture (T) and control (C) groups, meaning that the similarity between the two groups is greater than that among the different donors. This was also confirmed by the clear difference in the CA-plot (Figure 2A, right). However in the 15-day experiment (Figure 2B), the two main clusters do not always correspond to the co-cultured treatment (except for donors 3 and 5), but rather show that greater similarity among the samples from donors 1, 2, and 4 than between the co-culture and control groups. In the CA-plot for the 15-day experiment (Figure 2B, right), the data show a difference between the

two groups, but not as distinct as in the 5-day experiment. This result indicates that EC had larger genotype effects on MSC after 5 days of co-culture than after 15 days. Accordingly, it was not surprising that SAM analysis subsequently disclosed much more differentiated genes at 5 than at 15 days.

In summary, both the 5- and 15-day experiments showed that the data set was of good quality and no outliers were observed.

Differential expression analysis

In order to list the genes differentially expressed between the two groups, the 48803 genes were analyzed by SAM. Comparisons of gene expression between the control and co-cultured groups showed 285 genes with FDR less than 1% and fold-changes greater than 2 in the 5-day experiment, and 77 genes in the 15-day experiment.

The top 20 differentially regulated genes are shown in Table 2 i.e. from the whole genotype, these are the genes which had undergone the most pronounced changes. The dataset was also deposited in BASE. The top gene lists for the two different time points showed similar trends and shared some of the overrepresented genes (Table 2).

Classification of genes according to function

To explore and view functionally related genes together, the two overrepresented gene lists from the 5 and 15-day experiments were submitted to the DAVID database as separate sets of data. The 5-day gene lists were assessed by Gene Ontology and the pathway database. The data are presented in Table 3.

In the 5-day experiments, DAVID recognized a total of 218 specific gene symbols out of the list of 285 genes submitted. For the 218 genes identified by the Panther-BP-ALL databank, Gene Ontology (GO) analysis revealed 65 related GO terms. Table 3 presents the annotations of all the GO terms. The order in the list is based on the gene number involved. Some of the

GO terms (Signal peptide, Cell adhesion, Extracellular matrix, Blood vessel development, Cell migration, Response to wounding, ECM-receptor interaction, Mesenchymal cell development, Tube development, etc.) revealed very important bioinformatics about interactions between MSC and EC. At the same time, the pathway chart (Table 4) indicated the pathways most involved with the listed genes, such as ECM-receptor interaction, cell adhesion molecules (CAMs), TGF-beta signaling pathway, Leukocyte transendothelial migration and Focal adhesion. With respect to bone development, the most interesting disclosure was that 7 of the genes were involved in the TGF-beta pathway (Figure 3).

In the 15-day gene list, 65 specific gene symbols were identified by DAVID from a list of 78 differentiated genes. As shown in Figure 4, the 65 specific genes formed two GO clusters (cell-cell adhesion and GTP binding) on the basis of gene function. According to the KEGG-pathway database, the pathway map of the 15-day gene list disclosed 4 different pathways: Cell adhesion molecules (CAMs), Notch signaling pathway, Leukocyte transendothelial migration, and ECM-receptor interaction (Table 4B).

Validation microarray data by RT-PCR

mRNA levels of selected genes from MSCs cultured under mono-and coculture conditions for 5 and 15 days were confirmed by real time PCR (Figure 5). The relative expression levels are represented as MSC co-culture over monoculture. Thus, the gene expressions identified by microarray analysis were confirmed by a second method, real time PCR.

Discussion

Co-culture of MSC and EC is a promising strategy for bone tissue engineering [2]. The biological processes underlying cell-to-cell communication between MSC and EC are not well understood. The establishment of heterotypic cell contacts demonstrates that the co-culture system is a useful tool for studying paracrine and/or cell contact mediated interactions

between MSC and EC for application in bone tissue engineering. In the present study, the microarry method was applied for systematic analysis of patterns of global gene expression arising from cross-talk between MSC and EC and a map was generated of genes differentially expressed by MSC after co-culture with EC for 5 and 15 days. The dataset further classified the subsets of genes according to function, demonstrating that this classification reflected important hallmarks of physiological features of the effect of EC after different periods of co-culture.

Bidirectional gene regulation of angiogenesis and osteogenesis by co-culture

It has been shown that MSC can be induced into osteoblasts by addition of dexamethasone, ascorbic acid and beta-glycerophosphate [11], and can also be induced to form endothelial cells when the culture medium is supplemented with vascular endothelial growth factor [12]. The above studies indicated that an important feature of MSC is their multilineage differentiation potential. Under appropriate inductive conditions, MSCs are able to acquire characteristics of cells such as osteoblasts and endothelial cells. However, the molecular mechanisms that govern such MSC differentiation are not fully understood. The present co-culture model simulates *in vivo* conditions involving natural bone tissue and proved to be a useful model for exploring cellular induction.

The effects of co-culture on MSC included complex, bidirectional gene regulation mechanisms between MSC and EC. The top 20 gene list displayed those genes from the whole genotype which had undergone the most pronounced differentiation after co-culture. As shown in Table 2, co-culture resulted in upregulation of genes related to angiogenesis, such as von Willebrand factor (vWF), platelet/endothelial cell adhesion molecule-1 (PECAM1), cadherin 5 (CDH5), angiopoietin-related protein 4 (ANGPTL4), and cell surface antigen CD34. Also up-regulated in the cocultured-MSC were markers of osteogenesis, such as alkaline phosphatase (ALP), FK506 binding protein 5 (FKBP5) [13] and BMP. The list of

overrepresented genes demonstrated the bidirectional gene regulation of angiogenesis and osteogenesis after co-culture.

This finding could explain the results of a study in rats by Yu, et al., in which implantation of a polymer scaffold containing co-cultured EC and bone marrow-derived osteoblasts resulted in improved osteogenesis and enhanced vascularization [6]. This suggests a strategy for simultaneously improving angiogenesis and osteogenesis in engineered bone constructs. Further investigation of the molecular mechanisms underlying interactions between the two cell types might provide new insights into mesenchymal stem cell biology.

Angiogenic regulation might be mediated by cell-matrix interaction

Crosstalk between the two cell types affected not only cell-cell communication but also cell adhesion and cell-ECM communication. The list of top up-regulated genes also included ECM related genes, such as clusters of differentiation 93 (CD 93), cadherin 5 (CDH5), von Willebrand factor (vWF), and multimerin 1 (MMRN1). This trend was also noted in the cluster analysis. In the 5-day-experiment, GO clustering (Table 3) showed obvious effects on signal peptide (98 genes), cell adhesion (28 genes), ECM (27 genes), blood vessel development (18), cell migration (17 genes) and ECM-receptor interaction (10 genes). These data suggested that cell adhesion and cell-ECM interaction may play a crucial role in crosstalk between the two cell types through some signal process.

Extracellular matrix, secreted by the cells, could provide a local environment for cell-cell interactions through different signals, thereby affecting their differentiation. Previous study has shown that MSC cultured on EC-matrix undergoes EC differentiation and the study also indicated that EC-matrix contained certain signals and factors which could modify MSC differentiation into EC [14]. This conclusion is supported by the present study: the microarray data and the overrepresented expressions of angiogenic markers and ECM related genes after 5 and 15 days could also be explained by EC-matrix interactions.

TGF-beta pathway might be the mechanism of osteogenic induction

KEGG-Pathway mapping indicated several different pathways involved, such as the TGF-beta pathway, which is very important for osteogenesis differentiation and cell proliferation. Transforming growth factor-beta (TGF-beta) family members include TGF-betas, activins and bone morphogenetic proteins (BMPs) all secreted as cytokines and involved in multifunctional signaling. Interestingly, bone matrix is one of the richest reservoirs of TGF-beta and osteoblasts possess several different TGF-beta receptors [15]. Several studies have indicated that TGF-beta regulate osteoblast functions through their integrin receptors [15-17]. TGF-beta family members bind to the Type II receptor and recruit Type I, leading to activation of Type II receptor phosphorylates and Type I receptors. Once phosphorylated, receptors associate with the co-mediator, generate a heteromeric complex and then translocate into the nucleus. The specific genes will be activated by the complexes interacting with other DNA-binding and coactivator proteins. In the 5-day co-culture group, the following 7 genes were recruited to this pathway (Figure 3): BMP, follistatin (FST), v-myc myelocytomatosis viral related oncogene (c-Myc), inhibitor of DNA binding (Id), extracellular signal-regulated kinase (ERK), transcription factor (DP1), and cartilage oligomeric matrix protein (THBS1). Together theses genes contributed to most of the path from cell-to-cell interaction, the consequence being osteoblast differentiaion and cell cycle (Figure 3). This finding could explain and confirm the results of other previous studies, in which co-culture showed increased expression of bone markers (ALP, Col I) and positive effects on proliferation [4, 5]. This result suggests that EC could direct mesenchymal stem cells towards the osteoblastic phenotype and in a co-culture model, may be regarded as osteoinductive mediators [2]. TGF-beta pathway suppression could explain why only early stage bone markers were detected by our microarray data. Recently, experiments by Kyoko T, et al [18] proved that TGF-beta suppressed MSC differentiated into terminal osteoblasts and this effect could be reversed by

adding the TGF-beta inhibitors SB431542 and Ki26894. Using a different model and different methodology, this is confirmed by the microarray data in the present study.

In summary, whole gene profiling generated by microarray disclosed a complex process of the role of EC on MSC. Although in the present study a co-culture ratio of only 5:1 MSC/EC was used, a wide range of MSC genes and biological processes was significantly influenced by addition of less than 20% EC. These results may contribute to better understanding of bone physiology. In particular, the bidirectional gene regulation of angiogenesis and osteogenesis under co-culture conditions suggests new avenues for controlling and modulating bone-healing in tissue engineering, through cell-to-cell interactions. Further analysis is needed to determine the mechanisms underlying the bidirectional process. Functional validation is also needed.

Conclusions

This study has generated a global map of gene expression of the interaction between MSC and EC in a direct-contact model, which could be used to determine relative functional processes and pathways. The results showed a significant impact by EC on MSC after 5 and 15 days' co-culture, especially with respect to bidirectional gene regulation of angiogenesis and osteogenesis, through cell signalling, cell adhesion and cellular matrix. Cell-matrix interactions and TGF-beta signal pathways might play crucial roles in EC-induced gene regulation of MSC. Further analysis of the microarray data is warranted to explore these cellular and molecular interactions.

Acknowledgements

The authors would like to thank Kjell Petersen, Anne-Kristin Stavrum at the Department of Informatics for their assistance with J-express software and helpful discussions on bioinformatics. The authors also would like to thank Solveig Angelskår and Rita Holdhus at

the NMC Core Facility Laboratory, Bergen, for technical assistance with the microarray procedures and Dr. Joan Bevenius for language revision of the manuscript. This work was supported by The Research Council of Norway [(FRIMED, 17734/V50), (156744), (Stem Cell 180383/V40)]. All the microarray images from the scans were visually inspected by the staff at the NMC Core Facility Laboratory, Bergen.

References

1. Kneser U, Schaefer DJ, Polykandriotis E, Horch RE. Tissue engineering of bone: the reconstructive surgeon's point of view. *J Cell Mol Med* 2006;**10**:7-19.

2. Grellier M, Bordenave L, Amedee J. Cell-to-cell communication between osteogenic and endothelial lineages: implications for tissue engineering. *Trends Biotechnol* 2009;**27**:562-71.

3. Kanczler JM, Oreffo RO. Osteogenesis and angiogenesis: the potential for engineering bone. *Eur Cell Mater* 2008;**15**:100-14.

4. Villars F, Guillotin B, Amedee T, Dutoya S, Bordenave L, Bareille R, Amedee J. Effect of HUVEC on human osteoprogenitor cell differentiation needs heterotypic gap junction communication. *Am J Physiol Cell Physiol* 2002;**282**:C775-85.

5. Xue Y, Xing Z, Hellem S, Arvidson K, Mustafa K. Endothelial cells influence the osteogenic potential of bone marrow stromal cells. *Biomed Eng Online* 2009;**8**:34.

6. Yu H, VandeVord PJ, Mao L, Matthew HW, Wooley PH, Yang SY. Improved tissue-engineered bone regeneration by endothelial cell mediated vascularization. *Biomaterials* 2009;**30**:508-17.

7. Xing Z, Xue Y, Dånmark S, Schander K, Østvold S, Arvidson K, Hellem S, Finne-Wistrand A, Albertsson AC, K M. Effect of endothelial cells on bone regeneration using poly(L-lactide-co-1,5-dioxepan-2-one) scaffolds. *Journal of Biomedical Materials Research Part A (In press)* 2010.

8. Tusher VG, Tibshirani R, Chu G. Significance analysis of microarrays applied to the ionizing radiation response. *Proc Natl Acad Sci U S A* 2001;**98**:5116-21.

9. Dennis G, Jr., Sherman BT, Hosack DA, Yang J, Gao W, Lane HC, Lempicki RA. DAVID: Database for Annotation, Visualization, and Integrated Discovery. *Genome Biol* 2003;**4**:P3.

10. Huang da W, Sherman BT, Lempicki RA. Systematic and integrative analysis of large gene lists using DAVID bioinformatics resources. *Nat Protoc* 2009;**4**:44-57.

11. Jaiswal N, Haynesworth SE, Caplan AI, Bruder SP. Osteogenic differentiation of purified, culture-expanded human mesenchymal stem cells in vitro. *J Cell Biochem* 1997;**64**:295-312.

12. Oswald J, Boxberger S, Jorgensen B, Feldmann S, Ehninger G, Bornhauser M, Werner C. Mesenchymal stem cells can be differentiated into endothelial cells in vitro. *Stem Cells* 2004;**22**:377-84.

13. Liu TM, Martina M, Hutmacher DW, Hui JH, Lee EH, Lim B. Identification of common pathways mediating differentiation of bone marrow- and adipose tissue-derived human mesenchymal stem cells into three mesenchymal lineages. *Stem Cells* 2007;**25**:750-60.

14. Lozito TP, Taboas JM, Kuo CK, Tuan RS. Mesenchymal stem cell modification of endothelial matrix regulates their vascular differentiation. *J Cell Biochem* 2009;**107**:706-13.

15. Nesti LJ, Caterson EJ, Li WJ, Chang R, McCann TD, Hoek JB, Tuan RS. TGF-beta1 calcium signaling in osteoblasts. *J Cell Biochem* 2007;**101**:348-59.

16. Dallas SL, Sivakumar P, Jones CJ, Chen Q, Peters DM, Mosher DF, Humphries MJ, Kielty CM. Fibronectin regulates latent transforming growth factor-beta (TGF beta) by controlling matrix assembly of latent TGF beta-binding protein-1. *J Biol Chem* 2005;**280**:18871-80.

17. Lee JY, Kim KH, Shin SY, Rhyu IC, Lee YM, Park YJ, Chung CP, Lee SJ. Enhanced bone formation by transforming growth factor-beta1-releasing collagen/chitosan microgranules. *J Biomed Mater Res A* 2006;**76**:530-9.

18. Takeuchi K, Abe M, Hiasa M, Oda A, Amou H, Kido S, Harada T, Tanaka O, Miki H, Nakamura S, Nakano A, Kagawa K, Yata K, Ozaki S, Matsumoto T. Tgf-Beta inhibition restores terminal osteoblast differentiation to suppress myeloma growth. *PLoS One*;**5**:e9870.

Figure legands

Table 1 Donor information

FIG. 1 Box-plot of whole data set

A: Box-plot of the un-normalized data from 5-day experiment to the left, and un-normalized data from the 15-day experiment to the right. B: Box-plot of the quantile normalized data from the 5-day experiment to the left, and quantile normalized data from the 15-day experiment to the right.

A box plot is used to display the middle 50 % of the data points for each array, between the 25 and 75 percentiles. The horizontal line inside the box represents the median, which is the same as the 50 percentile. A line stretches out on either side of the box and it is determined by the interquartile range (IQR) which is defined as the difference between the 75 and 25 percentiles. The length of the lines is 1.5*IQR, and they start at the median. All data points inside the red lines are considered as non-outliers, while data points outside these limits are considered outliers of the distribution, i.e. extreme values, and are all marked with a separate black horizontal line.

FIG. 2 Global views of whole data set

A: Hierarchical Clustering (left) and Correspondence analysis plot (right) of samples from 5-days experiment, quantile-normalized data.

Relative similarity between each cluster elements: In the 5-day experiment hierarchical clustering of normalized data using Pearson Correlation as distance measure, there were two main clusters which correspond to the co-culture (T) and control (C) groups. No outliers are observed. In the CA plots the control group is displayed in pink, and the co-culture group in green. In the Correspondence Analysis plot for the 5-day experiment, there is a distinct

separation between the control group and the co-culture group, which indicates a differential expression of genes on the global level.

B: Hierarchical Clustering (left) and Correspondence analysis plot (right) of samples from 15-days experiment, quantile-normalized data.

In the 15-day experiment hierarchical clustering using Pearson Correlation as distance measure, gives two main clusters. These clusters do however not correspond to the biological groups, but rather show that the similarity between the samples from the same donor is larger than the similarity between the co-culture and control groups. In the Correspondence Analysis plot for the 15-day experiment, data show a separation between the control group and the co-culture group, but not as distinct as in the 5-day experiment.

Table 2 Top 20 up-or down- regulated genes by SAM

Table 3 Gene Ontology annotation of overrepresented gene lists by DAVID

FIG. 3 TGF signaling pathway

★ : Labeling showed 19 differentiated genes in the map

FIG. 4 15 days GO clustering by DAVID Database

Table 4: KEGG-Pathway map A: 5 days; B: 15 days

FIG. 5 Validation microarray data by RT-PCR

Table 1

Donor	Age	Gender	Code	Smoker	Taken Allergy <1 wk?	HIV,HBV,HCV
1	35	M	1429	Yes	No	Negative
2	24	M	1623	No	No	Negative
3	23	M	1637	No	No	Negative
4	24	M	1640	No	No	Negative
5	23	F	1641	No	No	Negative
6	34	F	1658	Yes	No	Negative

FIG. 1

A

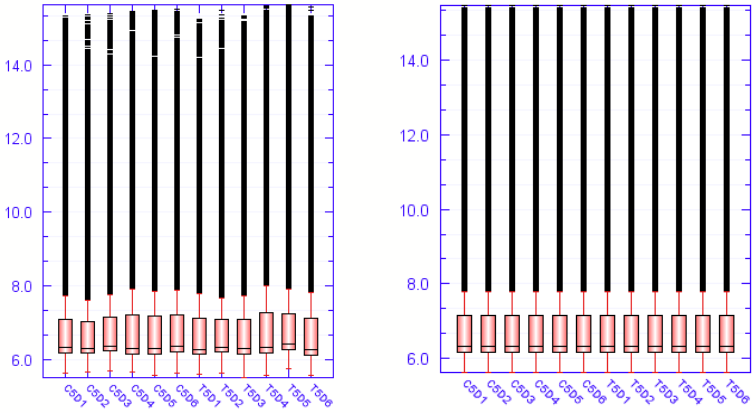
14.0
12.0
10.0
8.0
6.0
C501
C502
C503
C504
C505
C506
T501
T502
T503
T504
T505
T506

B

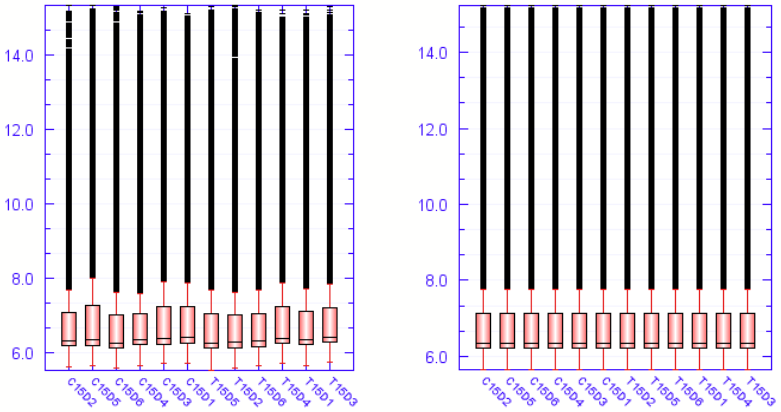
14.0
12.0
10.0
8.0
6.0
C1502
C1505
C1506
C1504
C1503
C1501
T1505
T1502
T1506
T1504
T1501
T1503

FIG. 2

A

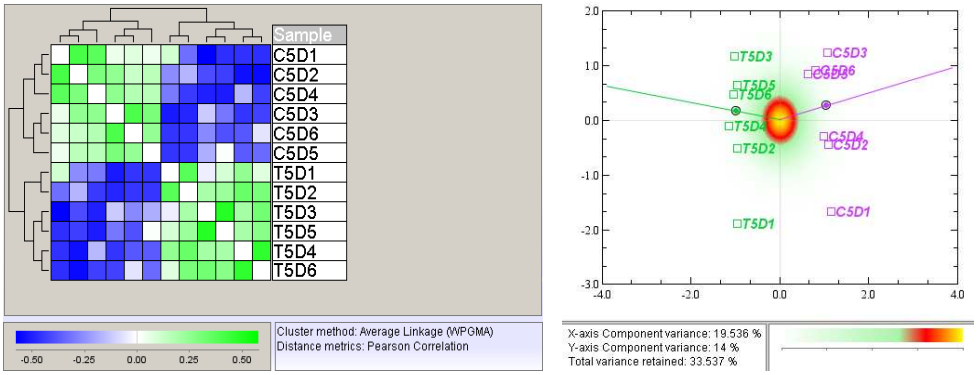
Sample
C5D1
C5D2
C5D4
C5D3
C5D6
C5D5
T5D1
T5D2
T5D3
T5D5
T5D4
T5D6
-0.50 -0.25 0.00 0.25 0.50
Cluster method: Average Linkage (WPGMA)
Distance metrics: Pearson Correlation
T5D3
C5D3
T5D5
T5D6
T5D4
C5D4
T5D2
C5D2
C5D1
T5D1
2.0 1.0 0.0 -1.0 -2.0 -3.0
-4.0 -2.0 0.0 2.0 4.0
X-axis Component variance: 19.536 %
Y-axis Component variance: 14 %
Total variance retained: 33.537 %

B

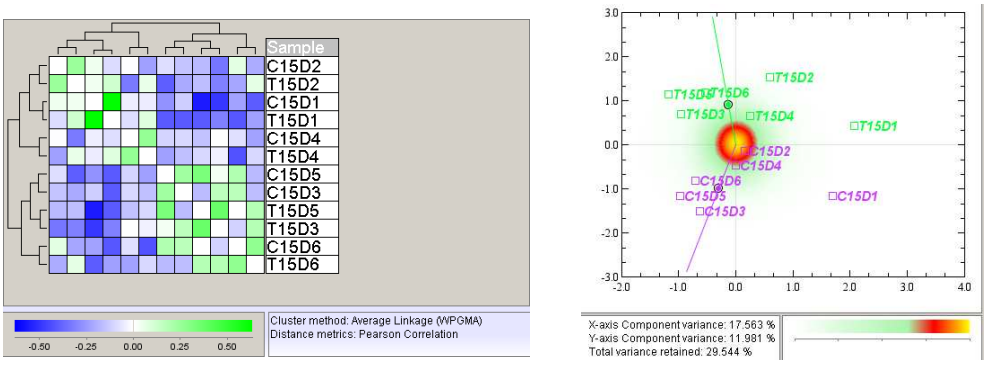
Sample
C15D2
T15D2
C15D1
T15D1
C15D4
T15D4
C15D5
C15D3
T15D5
T15D3
C15D6
T15D6
-0.50 -0.25 0.00 0.25 0.50
Cluster method: Average Linkage (WPGMA)
Distance metrics: Pearson Correlation
T15D2
T15D6
T15D3
T15D4
T15D1
C15D2
C15D4
C15D6
C15D5
C15D3
C15D1
3.0 2.0 1.0 0.0 -1.0 -2.0 -3.0
-2.0 -1.0 0.0 1.0 2.0 3.0 4.0
X-axis Component variance: 17.563 %
Y-axis Component variance: 11.981 %
Total variance retained: 29.544 %

Table 2

5 days

Up-regulated			
PROBE_ID	**Gene symbol**	**Fold Change**	**FDR[i]**
ILMN_1752755	VWF	100.664	0
ILMN_1704730	CD93	23.926	0
ILMN_1660114	MMRN1	14.994	0.237
ILMN_2071809	MGP	13.798	0.201
ILMN_1719236	CDH5	12.865	0
ILMN_1812968	SOX18	11.923	0
ILMN_1778444	FKBP5	11.398	0
ILMN_2142185	CLEC14A	10.417	0
ILMN_1651958	MGP	10.047	0.21
ILMN_2184373	IL8	9.954	0
ILMN_2313672	IL1RL1	9.2	0.224
ILMN_1748473	GIMAP4	7.819	0.282
ILMN_1701603	ALPL	7.811	0.655
ILMN_1675453	HHIP	7.166	0.333
ILMN_1658494	C13orf15	6.481	0
ILMN_1666733	IL8	6.44	0
ILMN_1663640	MAOA	6.386	0
ILMN_1754538	C10orf58	6.334	0.661
ILMN_1689518	PECAM1	6.288	0
ILMN_2411236	NRCAM	5.641	0
ILMN_1707727	ANGPTL4	5.569	0
Down-regulated			
ILMN_2134130	FLG	-21.279	0
ILMN_1813704	KIAA1199	-12.87	0
ILMN_1803213	MXRA5	-9.256	0
ILMN_1700081	FST	-8.503	0
ILMN_1810172	SFRP4	-8.081	0.187
ILMN_1730777	KRT19	-7.823	0
ILMN_1678842	THBS2	-6.88	0
ILMN_1720695	LOC730833	-6.79	0
ILMN_1734653	FNDC1	-6.261	0
ILMN_1667692	PTGIS	-6.095	0
ILMN_2163873	FNDC1	-6.079	0
ILMN_1726711	PENK	-5.907	0
ILMN_2200836	HSPB7	-5.584	0.267
ILMN_2385672	ELN	-5.516	0
ILMN_1677636	COMP	-5.473	0
ILMN_1678812	HAPLN1	-5.464	0
ILMN_1791447	CXCL12	-5.075	0
ILMN_1676663	TNFRSF11B	-5.002	0
ILMN_1699651	IL6	-4.942	0
ILMN_1665035	KRT14	-4.862	0
ILMN_1736760	KRT16	-4.837	0.195

15 days

Up-regulated			
PROBE_ID	**Gene Symbol**	**Fold Change**	**FDR[i]**
ILMN_1752755	VWF	62.564	0
ILMN_1704730	CD93	15.476	0
ILMN_1812968	SOX18	8.798	0
ILMN_1719236	CDH5	8.377	0
ILMN_2142185	CLEC14A	5.505	0
ILMN_1806733	COL18A1	4.625	0
ILMN_1660114	MMRN1	4.55	0
ILMN_1732799	CD34	4.543	0
ILMN_1689518	PECAM1	4.398	0
ILMN_2413158	PODXL	4.199	0
ILMN_1653466	HES4	4.18	0
ILMN_2341229	CD34	4.023	0
ILMN_1796288	COL5A3	3.706	0
ILMN_1668092	ESAM	3.671	0
ILMN_1752932	MPZL2	3.511	0
ILMN_1728785	GPR116	3.498	0
ILMN_1748473	GIMAP4	3.371	0
ILMN_2212878	ESM1	3.368	0
ILMN_1654324	HEYL	3.023	0
ILMN_1757440	FAM69B	2.936	0
ILMN_2371055	EFNA1	2.884	0
Down-regulated			
ILMN_2134130	FLG	-3.333	0
ILMN_1813704	KIAA1199	-2.725	0
ILMN_1678812	HAPLN1	-2.713	0
ILMN_1791447	CXCL12	-2.65	0
ILMN_2304512	SAA1	-2.579	0
ILMN_1689111	CXCL12	-2.453	0.837
ILMN_1733415	MFAP5	-2.424	0
ILMN_2376953	KCNK2	-2.253	0
ILMN_1810628	KIAA0367	-2.223	0
ILMN_1735910	VMO1	-2.179	0.35
ILMN_1719759	TNC	-2.163	0.814
ILMN_1765990	KCNK2	-2.145	0
ILMN_1656920	CRIP1	-2.141	0
ILMN_1801205	GPNMB	-2.056	0
ILMN_1805561	SLC14A1	-2.02	0.715

Table 3

5 days GO term Annotation

GO Term	Count	P Value	Fold Enrichment	Bonferroni	FDR	Enrichment Score
Signal peptide	98	1.16E-21	2.628575622	1.09E-18	1.82E-18	17.6667
Cell adhesion	28	7.02E-13	5.657907013	2.30E-10	9.51E-10	10.1803
Extracellular matrix	27	3.16E-12	5.450620082	6.35E-10	3.96E-09	9.15492
Blood vessel development	18	6.57E-08	5.183016488	1.08E-04	1.10E-04	6.70772
Cell migration	17	1.72E-06	4.362624794	0.00281331	0.002885	5.19
Response to wounding	22	9.51E-06	3.059008886	0.01546976	0.015965	3.64
Immunoglobulin domain	19	9.94E-06	3.469646478	0.00324597	0.01346	3..29
Hydroxylation	9	1.28E-06	11.21025606	4.20E-04	0.001737	3.22
EGF-like region, conserved site	17	1.35E-06	4.471613194	6.35E-04	0.001922	2.94
Chelation	4	8.97E-05	41.72706422	0.02889946	0.121339	2.83
Mesenchymal cell development	6	6.81E-04	8.439014025	0.67289333	1.137838	2.8
ECM-receptor interaction	10	1.36E-05	6.643437863	9.96E-04	0.014244	2.58
Domain:CTCK	4	0.00262892	14.25152905	0.91444934	4.039053	2.45
Response to organic substance	25	6.09E-05	2.480940351	0.09505084	0.102228	2.37
Regulation of locomotion	11	3.08E-04	4.168493974	0.39663103	0.516048	2.27
Prostaglandin receptor activity	3	0.00613438	24.53757225	0.90757121	8.186742	2.15
Urogenital system development	8	9.76E-04	5.087869325	0.79827397	1.626004	2.07
C-type lectin-like	7	0.00145361	5.6740638	0.49671796	2.05637	2.02
Tube development	10	0.00335422	3.29450998	0.99595457	5.486517	1.99
IL 17 Signaling Pathway	4	0.00518607	10.43809524	0.34712179	5.40332	1.9

FIG. 3

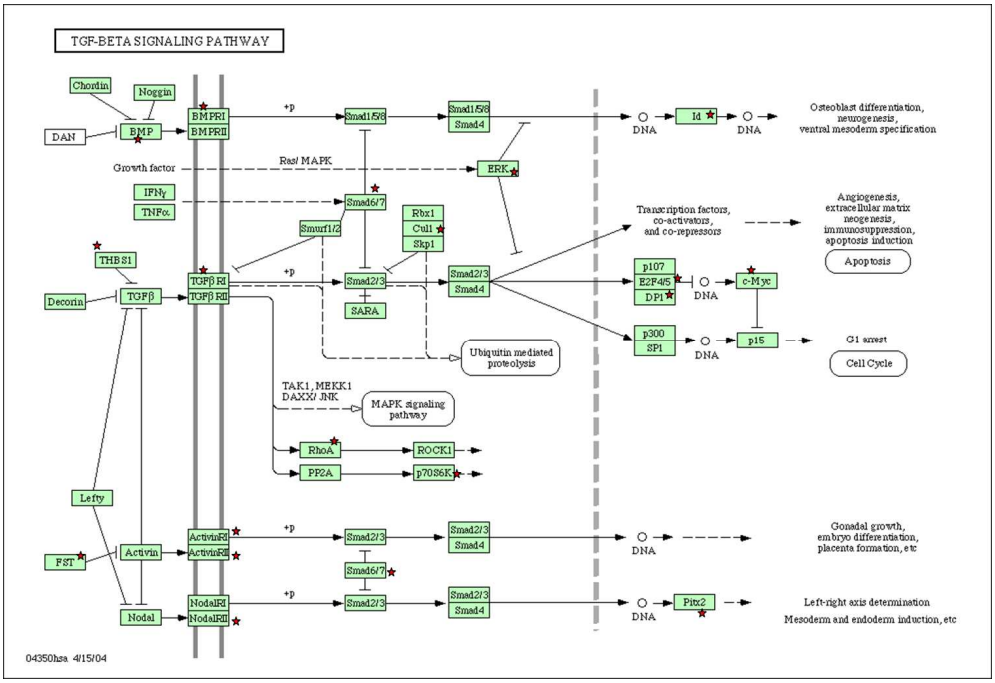
TGF-BETA SIGNALING PATHWAY
Chordin
Noggin
DAN
BMP
BMPRI
BMPRII
+p
Smad1/5/8
Smad1/5/8
Smad4
DNA
Id
DNA
Osteoblast differentiation,
neurogenesis,
ventral mesoderm specification
Growth factor
Ras/ MAPK
ERK
IFNγ
TNFα
Smad6/7
Rbx1
Cul1
Skp1
Smurf1/2
Transcription factors,
co-activators,
and co-repressors
Angiogenesis,
extracellular matrix
neogenesis,
immunosuppression,
apoptosis induction
Apoptosis
THBS1
Decorin
TGFβ
TGFβ RI
TGFβ RII
+p
Smad2/3
Smad2/3
Smad4
SARA
p107
E2F4/5
DP1
DNA
c-Myc
p300
SP1
DNA
p15
G1 arrest
Cell Cycle
Ubiquitin mediated
proteolysis
TAK1, MEKK1
DAXX/ JNK
MAPK signaling
pathway
RhoA
ROCK1
PP2A
p70S6K
Lefty
FST
Activin
ActivinRI
ActivinRII
+p
Smad2/3
Smad2/3
Smad4
DNA
Gonadal growth,
embryo differentiation,
placenta formation, etc
Smad6/7
Nodal
NodalRI
NodalRII
+p
Smad2/3
Smad2/3
Smad4
Pitx2
DNA
Left-right axis determination
Mesoderm and endoderm induction, etc
04350hsa 4/15/04

FIG. 4

Gene Functional Classification Result

Gene Group 1	Enrichment Score: 4.67388964559005
Gene Symbol	Gene Name
CD93	CD93 molecule
NRCAM	neuronal cell adhesion molecule
PLVAP	plasmalemma vesicle associated protein
PECAM1	platelet/endothelial cell adhesion molecule
CDH5	cadherin 5, type 2 (vascular endothelium)
CLEC14A	C-type lectin domain family 14, member A
GPNMB	glycoprotein (transmembrane) nmb
CLDN5	claudin 5
GPR116	G protein-coupled receptor 116
CD34	CD34 molecule
TM4SF18	transmembrane 4 L six family member 18
ESAM	endothelial cell adhesion molecule
MPZL2	myelin protein zero-like 2
PODXL	podocalyxin-like
PCDH17	protocadherin 17

Gene Group 2	Enrichment Score: 1.163038306137336
Gene Symbol	Gene Name
GIMAP8	GTPase, IMAP family member 8
GIMAP6	GTPase, IMAP family member 6
GIMAP7	GTPase, IMAP family member 7
GIMAP4	GTPase, IMAP family member 4

Table 4:

A: 5 days

Term	Count	P value	Genes
ECM-receptor interaction (hsa04512)	10	1.27E-05	VWF, SDC1, CD44, ITGA5, LAMA5, ITGA8, COMP, ITGA11, ITGA10, THBS2
Cell adhesion molecules (hsa04514)	10	4.19E-04	NRCAM, SDC1, CADM1, CD34, ITGA8, PECAM1, CLDN5, ESAM, ITGB2, CDH5
TGF-beta signaling pathway (hsa04350)	7	0.0039436	ID2, CDKN2B, ID1, COMP, FST, THBS2, BMP6
Leukocyte transendothelial migration (hsa04670)	7	0.0167636	PECAM1, CLDN5, ESAM, ITGB2, CXCL12, MMP2, CDH5
Focal adhesion (hsa04510)	9	0.0236411	VWF, ITGA5, LAMA5, ITGA8, COMP, ITGA11, ITGA10, THBS2, MYLK

B: 15 days

Term	Count	P value	Genes
Cell adhesion molecules (hsa04514)	6	3.80E-04	NRCAM, CD34, PECAM1, CLDN5, ESAM, CDH5
Notch signaling pathway (hsa04330)	4	0.0015182	MFNG, NOTCH4, JAG2, JAG1
Leukocyte transendothelial migration (hsa04670)	5	0.0024649	PECAM1, CLDN5, ESAM, CXCL12, CDH5
ECM-receptor interaction (hsa04512)	4	0.0079119	VWF, LAMA5, TNC, COL5A3

FIG. 5

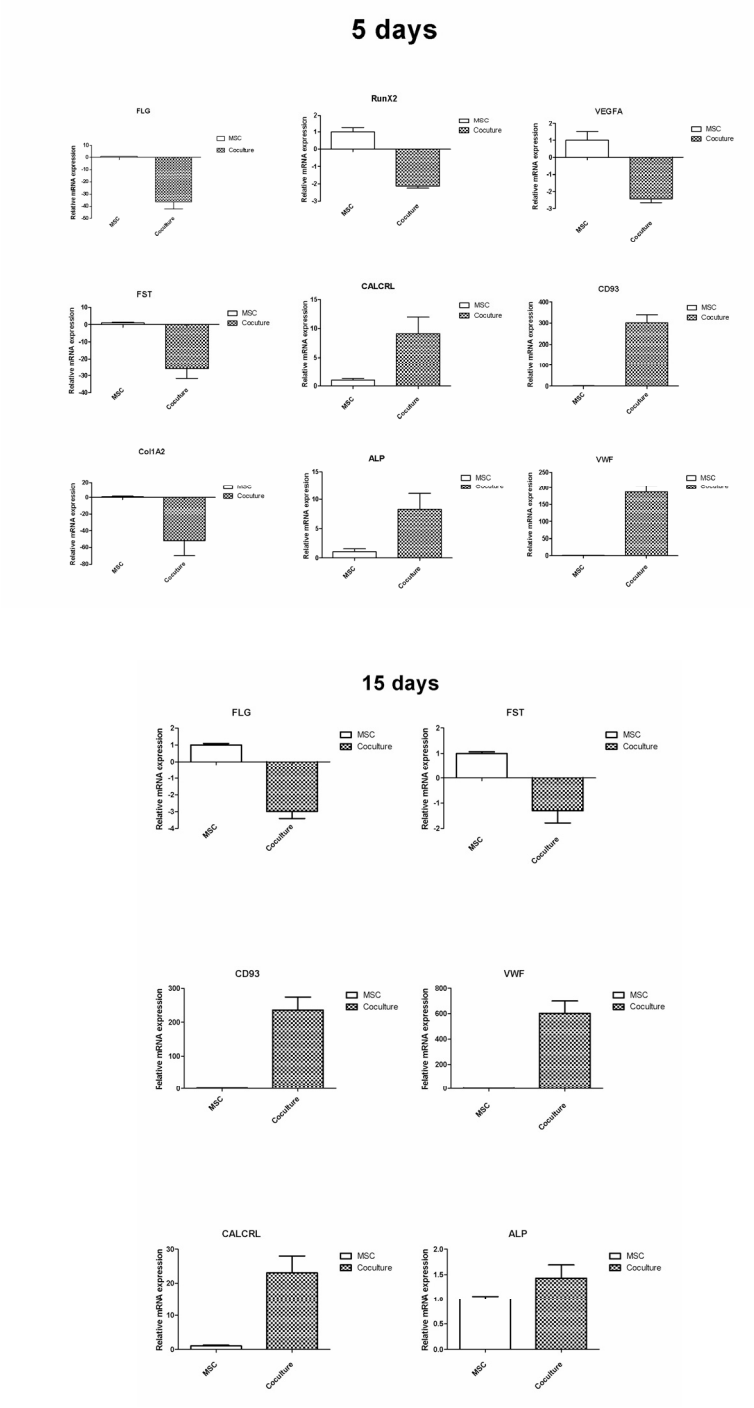
5 days
FLG
RunX2
VEGFA
FST
CALCRL
CD93
Col1A2
ALP
VWF
MSC
Coculture
Relative mRNA expression
15 days
FLG
FST
CD93
VWF
CALCRL
ALP
MSC
Coculture
Relative mRNA expression